Shan et al. *Zool. Res.* 2026, 47(1): 101−116
https://doi.org/10.24272/j.issn.2095-8137.2025.073
https://cstr.cn/32248.14.zr.2025.073

ZR | Zoological Research

Article Open Access

Diverse mitogenomic variations contribute to population differentiation in Eurasian tree sparrows (*Passer montanus*)

Cheng-Bin Shan[1,#], Ning Wang[1,2,#,*], Wei Liang[3], Xiang-Jiang Zhan[4,5], Long-Wu Wang[3], Le Yang[6], Qiong Liu[4,7], Yan-Lin Liu[8], Hao Meng[1], Hai-Tao Wang[9], Wei Xie[10], Sangeet Lamichhaney[11], Bin Liang[1,2,*]

[1] *State Key Laboratory of Reproductive Regulation and Breeding of Grassland Livestock*, *School of Life Sciences*, *Inner Mongolia University*, *Hohhot*, *Inner Mongolia Autonomous Region* 010070, *China*

[2] *Inner Mongolia Engineering Technology Research Center of Germplasm Resources Conservation and Utilization*, *Hohhot*, *Inner Mongolia Autonomous Region* 010070, *China*

[3] *Ministry of Education Key Laboratory for Ecology of Tropical Islands*, *Key Laboratory of Tropical Animal and Plant Ecology of Hainan Province*, *College of Life Sciences*, *Hainan Normal University*, *Haikou*, *Hainan* 571158, *China*

[4] *State Key Laboratory of Animal Biodiversity Conservation and Integrated Pest Management*, *Institute of Zoology*, *Chinese Academy of Sciences*, *Beijing* 100101, *China*

[5] *Key Laboratory of Animal Ecology and Conservation Biology*, *Institute of Zoology*, *Chinese Academy of Sciences*, *Beijing* 100101, *China*

[6] *Key Laboratory of Biological Resources and Biosafety*, *Institute of Plateau Biology Research of Xizang Autonomous Region*, *Lhasa*, *Xizang Autonomous Region* 850000, *China*

[7] *Life Science & Medicine*, *Northwest University*, *Xi'an*, *Shaanxi* 710069, *China*

[8] *College of Life Sciences*, *Qinghai Normal University*, *Xining*, *Qinghai* 810016, *China*

[9] *School of Life Sciences*, *Northeast Normal University*, *Changchun*, *Jilin* 130024, *China*

[10] *School of Life Sciences*, *Tsinghua University*, *Beijing* 100084, *China*

[11] *Department of Biological Sciences*, *Kent State University*, *Kent*, *Ohio* 44240, *USA*

ABSTRACT

Mitochondrial genomes (mitogenomes) play a crucial role in species adaptation to diverse evolutionary pressures. Although adaptive changes in mitochondrial genes have been reported under extreme conditions, large-scale analyses of mitogenomic evolution across ecologically diverse habitats are still limited. The Eurasian tree sparrow (*Passer montanus*), one of the most widely distributed avian species, occupies variable habitats, providing an ideal model for investigating mitochondrial responses to environmental heterogeneity. This study examined mitogenomic variation in tree sparrow populations sampled across China, revealing pronounced mitochondrial divergence in geographically isolated populations, particularly those in southern Xizang on the Qinghai-Xizang Plateau and the continental islands of Hainan and Taiwan. In the high-altitude population of southern Xizang, non-synonymous substitutions in *COX2* and *COX3* may enhance protein stability, potentially facilitating adaptation to cold and hypoxic conditions. In contrast, substitutions in *ATP6* (Hainan) and *ND5* (Taiwan) may reduce protein stability, implying distinct mitogenomic responses to local environmental constraints. Moreover, distinct tRNA mutations in the Hainan populations may confer increased structural flexibility, potentially contributing to island-specific adaptation. These findings highlight the role of mitochondrial genomes in responding to ecological variation and geographic barriers, underscoring the prospective functional consequences of mitogenomic evolution.

Keywords: Whole mitochondrial genomes; Eurasian tree sparrows; Geographical isolation; Genetic drift; Local adaptation

Received: 13 July 2025; Accepted: 15 September 2025; Online: 16 September 2025

Foundation items: This work was supported by the National Natural Science Foundation of China (32160114 and 32460125 to B.L., 32170460 and 32570495 to N.W., 32125005 to X.J.Z.), State Key Laboratory of Reproductive Regulation & Breeding of Grassland Livestock (2025KYPT0081), Young Science and Technology Talents Program for Universities in Inner Mongolia (NJYT23087) to B.L., Outstanding Young Scientist Project of Natural Science Foundation of Inner Mongolia Autonomous Region of China (2022JQ07) and Cultivation Project of Inner Mongolia University (21221505) to N.W., and Talent Research Startup Foundation of Hainan Normal University (HSZK-KYQD-202606) to L.W.W.

[#]Authors contributed equally to this work

*Corresponding authors, E-mail: ningwimu@imu.edu.cn; binliang@imu.edu.cn

INTRODUCTION

Mitochondria serve as bioenergetic hubs in eukaryotic cells, orchestrating oxidative phosphorylation, metabolic integration, and stress response signaling (Shen et al., 2022). Given their critical cellular functions (Roger et al., 2017), mitochondria have become a focal point in evolutionary biology and biomedical science. Mitochondrial DNA (mtDNA), in particular, is now widely used as a molecular marker for reconstructing phylogenetic relationships, tracing evolutionary processes, and investigating the etiology of various human diseases (Powell, 1994; Stewart & Chinnery, 2015; Wang et al., 2017). Beyond its utility in molecular systematics, the evolution of mitochondrial genomes (mitogenomes) has been increasingly associated with adaptive responses, especially in extreme environments under elevated energetic demand such as hypoxia or thermal stress (Ballard & Whitlock, 2004; Wallace, 2015).

Evidence from human populations has underscored the functional relevance of mitogenomic variation in thermogenesis and environmental adaptation. In high-altitude Sherpa populations from the southern mountainsides of the Himalayas, sequence variants in *ND1* (full gene names in Supplementary Table S1) have been implicated in physiological adjustments to chronic hypoxia (Kang et al., 2013). Similarly, associations between mitochondrial haplogroups and enhanced non-shivering thermogenesis in northern European populations (Wallace, 2015), along with temperature-associated mutations in *ND3* and *ATP6* (Balloux et al., 2009), suggest potential selective advantages for survival in cold environments. These findings establish a framework for broader exploration of mitogenomic adaptation across taxa exposed to harsh ecological pressures.

Mitogenomic adaptation to extreme environments has been documented across a range of vertebrate lineages. In high-altitude mammals, such as the Tibetan antelope (*Pantholops hodgsonii*), yak (*Bos grunniens*), Tibetan horse (*Equus caballus*), and golden snub-nosed monkey (*Rhinopithecus roxellana*), signatures of positive selection in *COX1*, *ND2*, and *ND6* suggest enhanced oxidative phosphorylation efficiency under hypoxic stress (Xu et al., 2005, 2007; Yu et al., 2011). Similarly, high-altitude Phasianidae birds show evidence of adaptive changes in *ND2*, *ND4*, and *ATP6*, which may support cold and oxygen-limited adaptation (Zhou et al., 2014). In the greater white-toothed shrew (*Crocidura russula*), variations in *ATP6*, *COX1*, and *ND1* have been linked to non-shivering thermogenesis in cold habitats (Fontanillas et al., 2005).

Despite these advances, most mitogenomic studies have focused on taxa inhabiting environmental extremes, such as high altitudes or cold regions, while species persisting across more ecologically variable or moderate habitats are comparatively understudied. This narrow taxonomic and environmental focus has created a significant knowledge gap in understanding how mitogenomes evolve under broader ecological contexts. Furthermore, cross-species comparisons, though informative, can be confounded by phylogenetic divergence and ecological differences (Monsanto et al., 2022; Ramos et al., 2018). In contrast, intraspecific analyses spanning wide geographic and environmental gradients offer a more direct framework for resolving the ecological and geographic drivers of mitogenomic divergence (Cheviron & Brumfield, 2009; Morales et al., 2015, 2018). However, such studies remain limited in scope and scale, particularly among non-model organisms with wide distributions and heterogeneous habitats (Vieira et al., 2024; Zhang et al., 2025).

The Eurasian tree sparrow (*Passer montanus*, hereafter referred to as “tree sparrow”) provides a powerful system for investigating mitogenome evolution across environmental gradients. As one of the most widespread and abundant avian species globally, the tree sparrow occupies a broad spectrum of habitats, including high-altitude plateaus, lowland plains, coastal basins, continental islands, forested mountains, and arid deserts, demonstrating remarkable ecological plasticity (Barlow et al., 2020). Taxonomically, tree sparrows are classified into nine subspecies (Clements et al., 2024), seven of which are present in China (Zheng, 2023). Populations across these regions exhibit pronounced variation in habitat type, which is reflected in differences in physiological traits, morphometric measurements (Sun et al., 2016; Xiong et al., 2020), and genetic structure (Qu et al., 2020), indicating ongoing environmental adaptation.

Although several studies have explored physiological and genomic responses to extreme environments in tree sparrows (Ding et al., 2021; Li et al., 2022; Qu et al., 2020), few have examined mitogenomic evolution across large geographic scales. The present study investigated mitogenomic diversity in tree sparrow populations spanning a wide range of habitats across China, aiming to identify signatures of population-specific adaptation. Two central questions were addressed: (1) Does mitogenomic divergence occur among geographically structured populations? (2) Do specific mitogenomic variants exhibit population specificity, and could these changes contribute to functional or evolutionary differentiation? Analyses focused on complete mitogenomes, complemented by comparison with two nuclear loci. This work contributes to a broader understanding of mitochondrial evolution and establishes a framework for future evolutionary and conservation research.

MATERIALS AND METHODS

Sample collection and data preparation

Blood and tissue samples were collected from tree sparrow populations spanning a wide range of geographic and ecological regions across China (Supplementary Tables S2, S3; Figure 1). Two house sparrows (*Passer domesticus*) from Xinjiang and Qinghai were included as outgroups. Genomic DNA was extracted using a TIANamp Genomic DNA Kit (TIANGEN Biotech, China) and stored in 120–150 μL of double-distilled water at −20°C.

Four-gene dataset for broad-scale geographic analysis: To characterize genetic structure across populations, two mitochondrial gene fragments (*CYTB* and *ND2*) were amplified from 208 individuals representing 33 populations (4–6 individuals per population; Supplementary Table S2). In parallel, two nuclear introns (*FGB5* and *PSMA2*; Supplementary Tables S1, S4) were amplified for comparative analysis. Polymerase chain reaction (PCR) amplifications were performed using a touchdown cycling protocol following Wang et al. (2016). Amplified products were purified using a QIAquick® PCR Purification Kit (QIAGEN N.V., Germany) and bidirectionally sequenced by BGI Genomics (Shenzhen, China). The resulting sequences provided a large-scale overview of genetic diversity and phylogeographic structure.

Whole mitogenomic data for fine-scale analysis: To enable detailed evolutionary inference, complete mitogenomes were

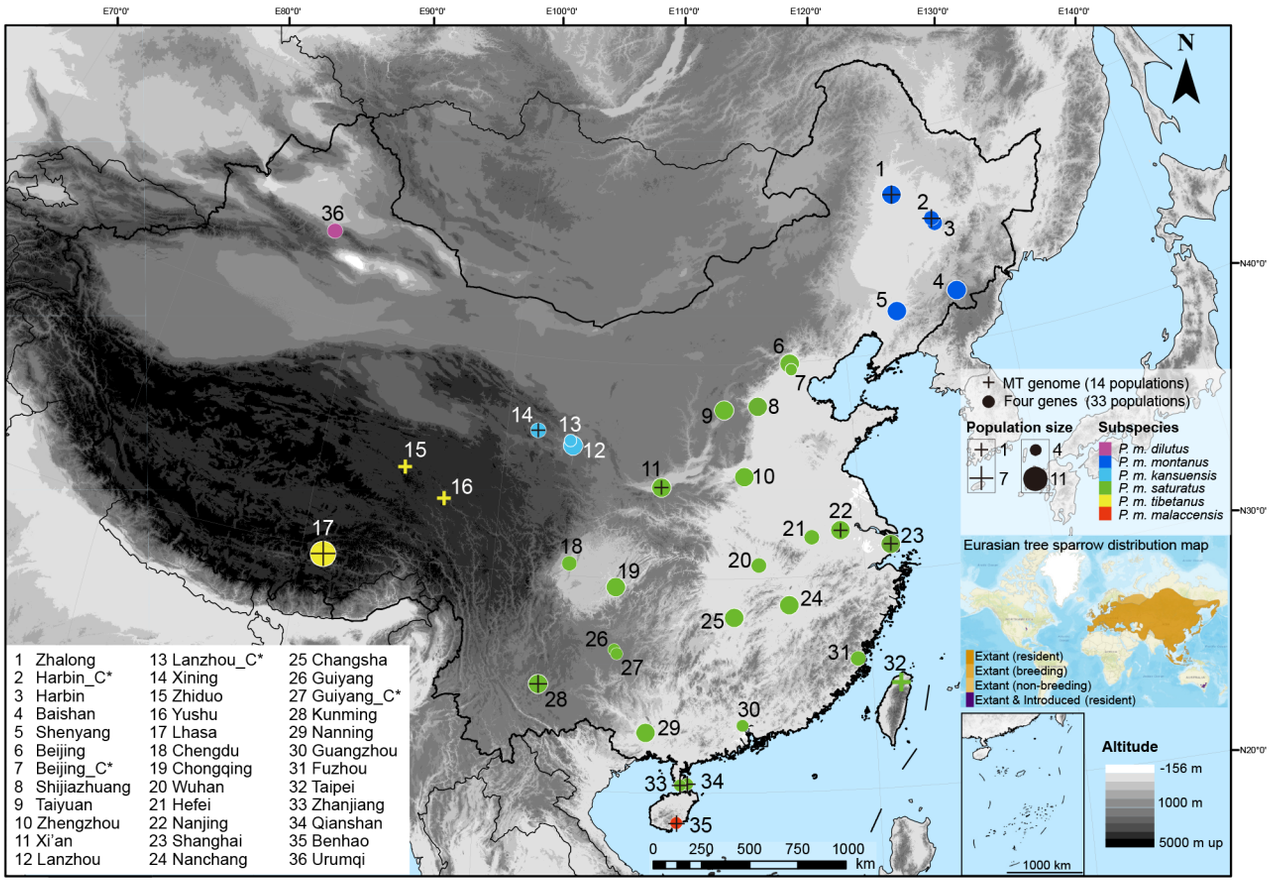

Figure 1 Sampling locations of Eurasian tree sparrows across China

Location names are indicated in the map legend. C* denotes location outside main cities. Subspecies (six of seven recognized in China; Zheng, 2023) associated with each region are indicated by different colors. Inset shows the distribution map of tree sparrows, downloaded from the IUCN Red List (https://www.iucnredlist.org/species/22718270/119216586#geographic-range).

obtained from 37 individuals representing 14 geographically diverse populations (Supplementary Table S3). Two house sparrows (GenBank: PQ783074 and PQ783112) served as outgroups. Entire mitogenomes were amplified using two overlapping long-range PCR fragments with primer sets listed in Supplementary Table S4 (Wang & Liang, 2016). This dual-fragment approach reduces the likelihood of nuclear mitochondrial (numt) sequence amplification (Liang et al., 2018), ensuring the integrity of the mitogenome assembly. PCR was carried out in a 40 μL system containing 20 μL of premix (Hi-performance Taq DNA polymerase, buffer, and dNTPs), 0.8 μL of forward and reverse primers (10 μmol/L each), 2 μL of DNA template (~100 ng/μL), and 16.4 μL of distilled water. Thermal cycling used a touchdown protocol with initial annealing at 58°C, decreasing by 0.5°C per cycle, followed by 10 cycles at 48°C.

Amplified fragments were sequenced on the Illumina HiSeq2000 platform (USA) at WX's laboratory (Tsinghua University, China), generating paired-end reads. Mitogenomes were assembled using Velvet (Zerbino & Birney, 2008) and Geneious Prime v.2019.2.1. All gene alignments were manually verified to confirm sequence integrity and the absence of unexpected stop codons. Final mitogenome assemblies were deposited in GenBank (Supplementary Table S3), GenBase (GB0006596), and the Science Data Bank (SDB, Data DOI: 10.57760/sciencedb.j00139.00252).

Four-gene dataset analysis

Summary statistics: For the two mitochondrial genes (*CYTB*, *ND2*) and nuclear introns (*FGB5*, *PSMA2*), the number of haplotypes (*N*), haplotype diversity (*Hd*), and nucleotide diversity (π) were calculated using DnaSP v.6 (Rozas et al., 2017). Nuclear sequences were phased prior to analysis (Stephens et al., 2001). Tajima's *D* (Tajima, 1989) and Fu and Li's D^* (Fu & Li, 1993) were calculated to test for selective neutrality.

Population differentiation: Population structure was evaluated using hierarchical analysis of molecular variance (AMOVA) in Arlequin v.3.5.2.2 (Excoffier & Lischer, 2010) with 10 000 permutations. Fixation indices (F_{ST}, Hudson et al., 1992) were estimated using the Weir & Cockerham (1984) method. Pairwise genetic differences, defined as the average number of base substitutions per site across sequence pairs, were calculated for concatenated mitochondrial (MT2) and concatenated nuclear (NUC2) datasets using MEGA11 (Tamura et al., 2021) with the Maximum Composite Likelihood model (Tamura et al., 2004) and gamma distribution of rate variation among sites.

To examine isolation-by-distance (IBD) and isolation-by-environment (IBE), partial Mantel tests (Smouse et al., 1986) were performed to assess correlations between genetic divergence and either geographic or environmental distances, controlling for the effect of the other factor. Population genetic distances were calculated as $F_{ST}/(1-F_{ST})$ (Rousset, 1997) for MT2 and NUC2 in Arlequin v.3.5.2.2. Geographic distances between populations were approximated as the shortest linear distances between sampling locations. Environmental

variables, including elevation and 19 bioclimatic factors, were retrieved from WorldClim v.2.0 (Cerasoli et al., 2022). Principal component analysis (PCA) was conducted using the 'prcomp' function in R to derive environmental distances (ENVALL) between sampling localities based on positions along the PC axes (Wang, 2013). For IBE, partial Mantel tests with 1 000 permutations were conducted using the "vegan" package in R, conditioning on geographic distance. Conversely, for IBD, ENVALL was used as the conditioning factor.

To reduce multicollinearity among environmental variables, ENMTools (Warren et al., 2010) was used to cluster the 20 variables based on predictors with absolute correlation coefficients greater than 0.8 (|r|>0.8), resulting in six groups. Maxent v.3.4.3 (Phillips et al., 2006) was then applied to select the top-contributing variable from each group based on its importance to the geographical distribution of tree sparrows. Six representative predictors were retained: elevation, Bio3 (isothermality), Bio4 (temperature seasonality), Bio12 (annual precipitation), Bio15 (precipitation seasonality), and Bio17 (precipitation of driest quarter) (Supplementary Tables S5, S6). Standardized Euclidean distances were computed among populations for each variable, and IBE was reassessed using the same procedures described above.

Genetic network and phylogenetic reconstruction: Individual-based, multilocus genetic networks were generated using the phased NUC2 dataset to visualize genetic structure. Pairwise distances were calculated under the HKY85 model, and networks were constructed using the Neighbor-Net algorithm (Bryant & Moulton, 2004) implemented in SplitsTree (Huson, 1998). Mitochondrial haplotype networks for *CYTB*, *ND2*, and MT2 were constructed using the TCS algorithm (Templeton et al., 1992) in PopART v.1.7 (Leigh et al., 2015).

Maximum-likelihood (ML) phylogenies were inferred for individual mitochondrial (*CYTB*, *ND2*) and nuclear (*FGB5*, *PSMA2*) gene segments, as well as the concatenated datasets (MT2 and NUC2), using RAxML v.7.2.6 (Stamatakis, 2006) under the GTR+Γ model, with 1 000 bootstrap replicates for node support. Bayesian phylogenetic trees for the concatenated datasets were generated using MrBayes v.3.1.2 (Ronquist & Huelsenbeck, 2003), with gene-specific substitution models selected using jModelTest v.2.1.10 (Darriba et al., 2012) based on Akaike Information Criterion (AIC; Supplementary Table S7). Each analysis consisted of two independent runs of four Monte Carlo Markov chains (MCMCs) for 100 million generations, with trees sampled every 10 000 generations. The initial 25% of samples were discarded as burn-in, and all-compatible consensus trees were constructed with posterior probability (PP) support values. Samples from Taiwan (n=4) and southern Qinghai (Yushu and Zhiduo, n=2) were collected exclusively for whole mitogenome sequencing; their *CYTB* and *ND2* gene segments were thus extracted and incorporated into the mitochondrial network and phylogenetic analyses.

Mitogenome data analyses

Genetic differentiation and phylogenetic inference: Whole mitogenome sequences from 37 individuals were analyzed as two datasets: the complete mitogenome and a reduced dataset comprising 15 genes (13 protein-coding genes (PCGs) and two rRNA genes; MT15). For both datasets, pairwise genetic distances, defined as the number of base substitutions per site, were calculated using the Maximum Composite Likelihood model in MEGA11 (Tamura et al., 2004) and visualized as heatmaps. AMOVA was performed separately for each of the 15 genes using Arlequin v.3.5.2.2, and a haplotype network based on the MT15 dataset was constructed in PopART v.1.7. Phylogenetic trees for the entire genomes and concatenated MT15 dataset were reconstructed using both ML and Bayesian methods, following the procedures described above.

Divergence time estimation and demographic history: Bayesian Coalescent Skyline plots and time calibration were conducted in BEAST v.2.5.3 (Bouckaert et al., 2019) using the MT15 dataset to infer divergence times and historical population dynamics. Each gene was assigned its best-fit or closely related substitution model, and a strict molecular clock was applied with a mean substitution rate of 1.6×10^{-9} substitutions/site/year, averaged across the 15 mitochondrial genes (Arcones et al., 2021). Divergence between the tree sparrow and house sparrow was constrained using a secondary calibration of 5 million years ago (4–6 Ma) (Päckert et al., 2021). Three independent MCMC runs were conducted for each analysis, each exceeding 3×10^{7} generations. Convergence and effective sample sizes (ESS>200) were assessed using Tracer v.1.7.2 (Rambaut et al., 2018).

Selection and structural analysis

Site-level variation: To investigate mutational patterns potentially contributing to population divergence, variation across all 13 PCGs, 22 tRNAs, and two rRNAs was analyzed. For each gene alignment, ancestral sequences were reconstructed using RAxML-NG (Kozlov et al., 2019) with the '--ancestral' option, designating *P. domesticus* as the outgroup. Substitution models were set to GTR for tRNAs and selected based on model testing (Supplementary Table S7). Substitutions were identified by comparison with the inferred ancestral sequences, and the proportions of transitions and transversions were calculated for each population. For PCGs, synonymous (K_s) and nonsynonymous (K_a) substitutions were distinguished. Following Zhang et al. (2014), population-specific sites (PSSs) were defined as substitutions fixed within a population but absent from others. In addition, non-perfect population-specific K_a sites were identified as K_a substitutions present in all individuals of a population but also present in a single individual outside that population.

Selection detection: Populations from Xizang (Dangxiong, Lhasa), Hainan (Benhao, Lingshui), and Taiwan (Taipei) formed distinct clusters in MT15 analyses and were selected as focal groups for detection of adaptive evolution. To evaluate potential selection across the 13 mitochondrial PCGs, codeml from PAML v.4.9 (Yang, 2007) was used to estimate the ratio of nonsynonymous to synonymous substitution rates ($\omega=d_N/d_S$), a standard metric of selective pressure, with ω<1, =1, and >1 indicating purifying selection, neutral evolution, and positive selection, respectively. However, average ω across all sites and lineages is rarely greater than 1, as positive selection typically acts on a subset of sites or lineages (Yang, 2007). Accordingly, branch and branch-site models were applied to detect localized signals of positive selection.

For the branch models (Yang, 1998), the null hypothesis (H_0) assumed a uniform ω value across all clades, while the alternative hypothesis (H_1) allowed different ω values for the

foreground branch (one of the focal Xizang, Hainan, or Taiwan populations) and background branches (remaining populations). Positive selection was then inferred when $\omega_{foreground}>1$ and the likelihood ratio test (LRT; df=1) supported H_1 ($P<0.05$). For the branch-site models (Nielsen & Yang, 1998), ω varied among protein sites and across branches. The null hypothesis fixed ω at 1 along the foreground branches (Xizang, Hainan, or Taiwan), while the alternative allowed a subset of sites to evolve under $\omega>1$. Both hypotheses have background branches modeled under two site classes: purifying selection ($0<\omega_0<1$) or neutral evolution ($\omega_{1=}1$) (Yang et al., 2005). Analyses were conducted using the rooted Bayesian species tree inferred from the concatenated MT15 dataset (Álvarez-Carretero et al., 2023).

Given the potential for reduced statistical power of LRT in branch-site models due to complex parameterization (Yang & dos Reis, 2011), Bayes Empirical Bayes (BEB) inference was also used to identify codon sites with elevated posterior probabilities of positive selection. Sites with BEB posterior probabilities >0.95 were considered strong candidates, while those >0.5 were considered suggestive (Álvarez-Carretero et al., 2023).

To assess whether mitochondrial PCGs experienced shifts in selective pressure associated with population occupying distinct environmental conditions, RELAX analyses were performed in HyPhy (Wertheim et al., 2015; Kosakovsky Pond et al., 2020). This method evaluates whether selective pressure is relaxed or intensified along designated foreground branches by estimating the parameter k, which reflects a contraction ($k<1$) or expansion ($k>1$) of the ω distribution toward or away from neutrality ($\omega=1$). Each focal group (Xizang, Hainan, or Taiwan) was tested as the foreground against the remaining populations as background, and significance was evaluated via likelihood ratio tests.

Structural prediction and functional assessment: Several nonsynonymous substitutions and candidate sites under potential positive selection were identified as population-specific in Hainan, Taiwan, or Xizang populations. To evaluate their potential contribution to population differentiation, protein-level impacts of these variants were examined through comparative structural analyses. Subunits associated with the COX complex were all included in the structure prediction to examine the effect of site variation on subunit interactions. Protein structures were predicted using AlphaFold2 (Jumper et al., 2021) and AlphaFold2-multimer (Evans et al., 2021), with homologous sequence alignments generated via MMseqs2 (Mirdita et al., 2019) and HHsearch (Steinegger et al., 2019). PyMOL v.1.2 (Delano, 2002) was used for visualization and calculating polarity and bond lengths. Electrostatic surface potentials near the mutation site were also predicted using the Adaptive Poisson-Boltzmann Solver (APBS) plugin (Jurrus et al., 2018).

In parallel, population-specific changes in tRNAs were analyzed at both secondary and tertiary structural levels. Secondary structures were predicted using the MXfold2 server (Sato et al., 2021), while 3D structures were modeled with 3dRNA v.2.0 (Zhang et al., 2022). Electrostatic surface potentials of RNA 3D structures were also calculated using the APBS plugin in PyMOL.

RESULTS

Genetic diversity and population structure across mitochondrial and nuclear loci

Two mitochondrial gene segments (*CYTB* and *ND2*, totaling 1 534 bp) and two nuclear introns (*FGB5* and *PSMA2*, totaling 733 bp) were analyzed to assess genetic variation across populations. All loci exhibited high haplotype diversity (>0.5), while nucleotide diversity (π) was relatively low in the mitochondrial genes (Table 1). Neutrality tests based on Tajima's D and Fu and Li's D^* suggested contrasting evolutionary patterns: nuclear loci conformed to expectations under neutral evolution, whereas significantly negative values in mitochondrial genes indicated possible selective or demographic influences (Table 1).

AMOVA revealed that most genetic variation occurred within populations for all four genes. However, mitochondrial loci exhibited substantially higher among-population differentiation ($F_{ST}>0.15$) compared to nuclear loci ($F_{ST}<0.05$; Table 2). This disparity suggests that mitochondrial divergence among sparrow populations may be more pronounced than nuclear divergence, although the short lengths of nuclear sequences may limit their resolution. Further analysis using the MT15 dataset revealed consistently elevated among-population variation and F_{ST} values across all mitochondrial genes, reinforcing the presence of pronounced mitogenomic divergence among populations (Table 2).

Genetic structure and divergence patterns across data types

Patterns of population structure in tree sparrows varied markedly between mitochondrial and nuclear datasets. Mitochondrial data (MT2) revealed greater population-level divergence (Supplementary Figure S1A), with haplotype networks highlighting the distinctiveness of the Hainan and Xizang populations (Supplementary Figure S2). However, mitochondrial genetic distance showed no significant correlation with geographic distance (IBD: r=−0.04, P=0.63) but was significantly associated with overall environmental variation (IBE-ENVALL: r=0.201, P=0.007). Among individual environmental variables, elevation showed a significant correlation with mitochondrial divergence (r=0.4, P=0.025). In contrast, nuclear divergence exhibited no significant relationship with either geographic distance (IBD: r=0.095, P=0.160) or overall environmental variation (IBE-ENVALL: r=0.114, P=0.114), although isothermality (Bio3) and elevation had significant individual effects (Supplementary Table S6).

Table 1 Summary of four genes across all tree sparrow samples

Type	Gene	N_1	N_2	Nh	Hd	π	k	S	Tajima's D	Fu and Li's D^*
MT	*CYTB*	205	589	44	0.795	0.003	1.356	38	−2.308**	−4.044**
	ND2	203	945	96	0.969	0.004	3.491	97	−2.442**	−6.322**
NUC	*FGB5*	207	403	34	0.596	0.006	2.355	25	−1.047	−0.993
	PSMA2	206	330	43	0.889	0.015	5.036	33	−0.137	−1.879

N_1: Number of individuals; N_2: Total number of sites; Nh: Number of haplotypes; Hd: Haplotype diversity; π: Nucleotide diversity; k: Average number of nucleotide differences; S: Number of segregating sites. *: $P<0.05$; **: $P<0.01$.

Table 2 AMOVA results for geographic populations of tree sparrows

Gene/pop.	Among populations			Within populations			F_{ST}
	Sum of squares	Variance components	Percentage of variation	Sum of squares	Variance components	Percentage of variation	
For MT2 and NUC2 datasets							
CYTB/33[a]	39.81	0.11	15.90	98.48	0.57	84.10	0.16**
ND2/33	103.74	0.29	16.51	248.83	1.46	83.49	0.17**
FGB5/33	42.31	0.01	1.04	436.99	1.17	98.96	0.01
PSMA2/33	125.56	0.12	4.59	909.38	2.40	95.41	0.05**
For MT15 dataset							
12S/14[a]	6.82	0.16	55.63	2.86	0.12	44.37	0.56**
16S/14	14.34	0.34	59.39	5.33	0.23	40.61	0.59**
ATP6/14	21.34	0.41	41.38	13.42	0.58	58.62	0.41**
ATP8/14	4.24	0.09	48.56	2.19	0.09	51.44	0.49*
COX1/14	33.79	0.65	40.94	21.50	0.93	59.06	0.41**
COX2/14	34.16	0.79	56.35	14.00	0.61	43.65	0.56**
COX3/14	16.45	0.37	53.60	7.33	0.32	46.40	0.54**
CYTB/14	36.29	0.81	53.80	16.08	0.69	46.20	0.54**
ND1/14	17.79	0.18	16.20	21.02	0.91	83.80	0.16*
ND2/14	49.64	1.15	57.52	19.61	0.85	42.48	0.58**
ND3/14	9.89	0.18	38.29	6.75	0.29	61.71	0.38**
ND4/14	44.08	0.95	49.63	22.08	0.96	50.37	0.49**
ND4L/14	8.41	0.17	46.01	4.67	0.20	53.99	0.46**
ND5/14	44.23	0.68	29.40	37.79	1.64	70.60	0.29**
ND6/14	14.93	0.33	52.60	6.86	0.29	47.40	0.53**

[a]: 33 and 14 denote number of tree sparrow populations sampled for each dataset. MT15 dataset, comprising two rRNAs and 13 mitochondrial protein-coding genes, was collected from 14 Eurasian tree sparrow populations. MT2 dataset (*CYTB* and *ND2*) and NUC2 dataset (*FGB5* and *PSMA2*) were sampled from 33 populations. F_{ST}: Fixation Index. *: $P<0.05$; **: $P<0.01$.

Moreover, the NUC2 dataset failed to resolve discrete population clusters (Supplementary Figure S3), possibly due to the limited resolution of the two short nuclear introns analyzed.

Analysis of the expanded MT15 dataset revealed pronounced genetic divergence across individuals, with Taiwan in addition to Xizang and Hainan forming distinct lineages (Supplementary Figure S1B). The MT15 haplotype network reinforced these patterns, showing well-defined clades corresponding to each of the three populations (Figure 2A).

Phylogenetic analysis highlights population-level divergence

Phylogenetic reconstructions based on mitochondrial markers revealed pronounced population structure, in contrast to patterns inferred from nuclear loci. Specifically, Bayesian and ML trees constructed from the concatenated nuclear dataset (NUC2) showed no clear population structure (Supplementary Figure S4; tree file). Conversely, mitochondrial trees based on the MT2 dataset resolved distinct clades for the Hainan and Xizang populations, although support for the Hainan clade was weaker (PP=0.95, BS=59) than for the Xizang clade (PP=0.98, BS=89; Supplementary Figure S5; tree file).

Mitogenome-wide analyses further reinforced this pattern. Bayesian phylogenies derived from the MT15 dataset recovered three strongly supported clades corresponding to Hainan, Xizang, and Taiwan (PP>0.95). In this tree, the Hainan clade diverged earliest, followed by Xizang, while the Taiwan clade was nested within the remaining populations (Figure 2B). The ML tree based on MT15 recovered the same focal clades, although the branching order differed and node support was weaker (Supplementary Figure S6A). Similarly, the ML and Bayesian trees based on the complete mitogenome strongly supported the focal clades, with some topological variations observed among weakly supported branches (Supplementary Figure S6; tree file). Given the congruence across datasets, subsequent interpretation focused on results from the MT15 analyses.

Bayesian divergence time estimates based on MT15 indicated that the crown clade diversified approximately 0.2 Ma (95% HPD: 0.15–0.26), with population-specific divergence events for Hainan, Xizang, and Taiwan dated to approximately 0.024 Ma (95% HPD: 0.0074–0.0442), 0.022 Ma (95% HPD: 0.0105–0.039), and 0.028 Ma (95% HPD: 0.0137–0.0475), respectively (Supplementary Figure S6B). These divergence times coincide with the Last Glacial Maximum (LGM; Clark et al., 2009). Despite glacial-era climatic instability, tree sparrow populations remained stable, with no evidence of recent expansions or bottleneck events (Supplementary Figure S7).

Mitogenomic variation and population-specific substitutions

Genetic variation across all mitochondrial genes (13 PCGs, two rRNAs, and 22 tRNAs) was examined relative to reconstructed ancestral sequences. Among the PCGs, 294 nucleotide substitutions were identified, comprising 279 transition sites and 15 transversion sites. Of these, 31 were nonsynonymous (K_a) and 263 were synonymous (K_s). Substitution rates, defined as the average number of substitutions among populations, were highest in *COX3*, *CYTB*, and *ND2*, while *ATP8*, *ND3*, and *ND4L* displayed the most heterogeneous substitution patterns across populations (Figure 3A).

In non-coding RNA genes, 28 variable sites were detected, including two transversions, 20 transitions, four insertions, and two deletions, with an uneven distribution across rRNA and

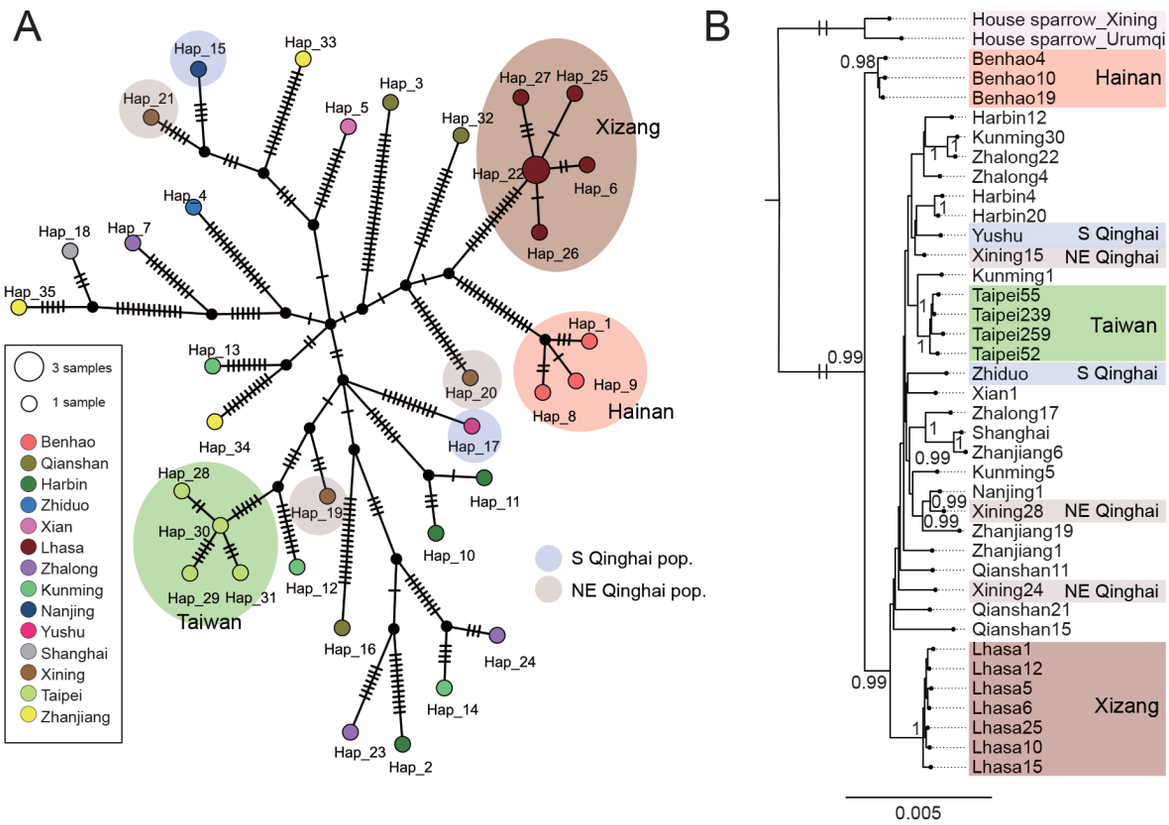

Figure 2 Network and species tree based on 15 concatenated mitochondrial genes (MT15 dataset)

A: Haplotype network. "Hap" refers to haplotype. Hap_15 (Zhiduo) and Hap_17 (Yushu) originated from South (S) Qinghai population; Hap_19, Hap_20, and Hap_21 were from Xining in northeastern (NE) Qinghai. B: Bayesian species tree. ML tree using the same dataset showed a similar divergence pattern (Supplementary Figure S6). Hainan (Benhao), Taiwan (Taipei), and Xizang (Lhasa) populations formed distinct clades, as highlighted in the figure. Samples from Zhiduo, Yushu (S Qinghai), and Xining (NE Qinghai) are also highlighted. Posterior probabilities (PP)>0.95 are indicated at corresponding nodes. House sparrow (*Passer domesticus*), collected from Xining and Urumqi, served as an outgroup.

tRNA loci (Figure 3B).

Distinct population-specific substitution patterns were observed in the Hainan, Taiwan, and Xizang populations (Figure 3C), with multiple variants shared among all sampled individuals within each group (Supplementary Table S8). In Hainan, 18 PSSs were identified across nine PCGs and three tRNAs ($tRNA^{Asp}$, $tRNA^{Cys}$, and $tRNA^{Phe}$). The Taiwan population was characterized by four population-specific K_s sites distributed across four PCGs. In Xizang, 13 PSSs were detected in eight PCGs, 16S rRNA, and $tRNA^{Asp}$, including population-specific K_a sites in *COX2* and *COX3* (Supplementary Table S8; Figure 3D).

Mitogenomic selection patterns across focal populations

Branch model analyses indicated putative signals of positive selection in *ATP6* (Hainan, *P*=0.01), *COX3* and *ND1* (Xizang, *P*=0.03), and *ND5* (Taiwan, *P*=0.04) (Supplementary Table S9), with *COX3* exhibiting population-specific K_a in Xizang, and *ATP6* and *ND5* harboring non-perfect population-specific K_a variants (Figure 3C). Although these *P*-values did not meet the threshold for significance following stringent Bonferroni correction (Shaffer, 1995), the biological relevance of these genes—given their functional roles and population-specific patterns—warrants further consideration. The branch-site model did not yield significant evidence of positive selection based on the LRT results. Nevertheless, BEB analysis identified several amino acid (aa) residues with evidence of selection ($Pr_{[\omega>1]}$>0.5), including ATP8-aa46 (Ser, $Pr_{[\omega>1]}$=0.751) in Hainan; COX2-aa74 (Thr, $Pr_{[\omega>1]}$=0.637), COX3-aa135 (Thr, $Pr_{[\omega>1]}$=0.944), and ND1-aa270 (Thr, $Pr_{[\omega>1]}$=0.547) in Xizang; and CYTB-aa331 (Thr, $Pr_{[\omega>1]}$=0.833), ND5-aa44 (Ala, $Pr_{[\omega>1]}$=0.829), and ND5-aa193 (Tyr, $Pr_{[\omega>1]}$=0.552) in Taiwan (Supplementary Table S10). However, some of these substitutions were found in only a single individual (e.g., CYTB-aa331; Figure 3D) or corresponded to non-perfect population-specific K_a sites (e.g., ATP8-aa46; Figure 3D). RELAX analysis revealed significant relaxed selection in *CYTB* in the Taiwan population (k=0; *P*<0.05), while no significant relaxation or intensification was detected for other genes or populations (Supplementary Table S11).

Structural and functional consequences of population-specific mutations

Impact of mutations on protein-coding genes: To assess the evolutionary significance of PCGs in focal populations, structural analyses were conducted for *ATP6*, *ATP8*, *COX2*, *COX3*, and *ND5* harboring population-specific K_a sites. All protein structures predicted by AlphaFold exhibited high reliability, with local distance difference test (LDDT) scores exceeding 80%. In the Xizang population, aa substitutions in *COX2* (aa74: Met→Thr) and *COX3* (aa135: Ala→Thr) were predicted to increase protein stability through the formation of additional hydrogen bonds with adjacent residues (Balcão & Vila, 2015; Figure 4A). In contrast, substitutions in *ATP6* (aa195: Val→Ala, Hainan) and *ND5* (aa193: Cys→Tyr; Taiwan) were predicted to reduce structural stability by disrupting hydrogen bond interactions, such as the loss of

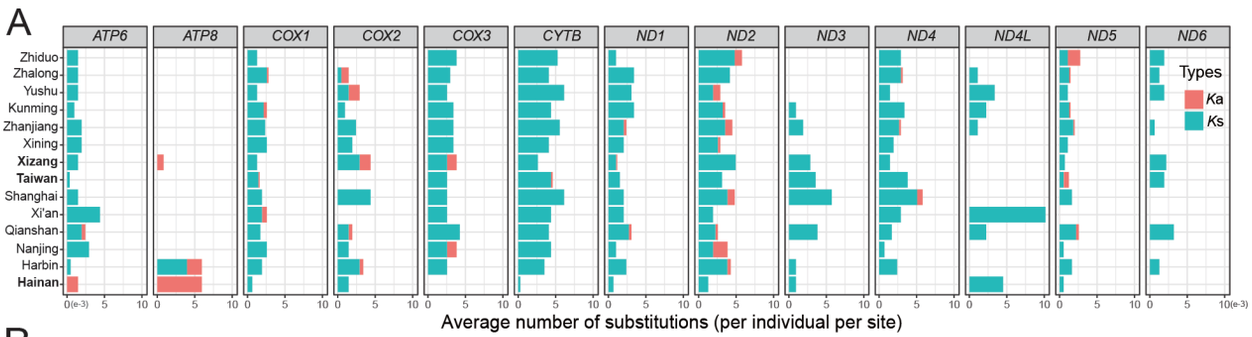

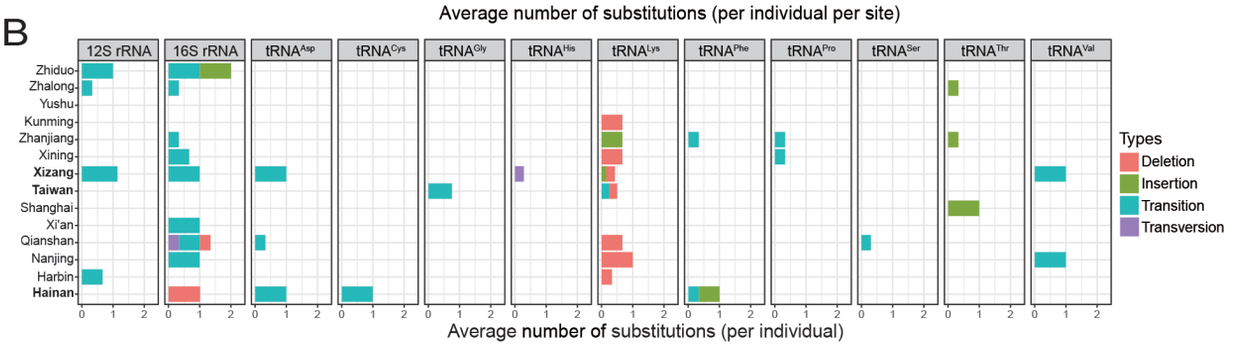

C

	a			b			c		
Site	1	2	3	4	5	6	7	8	9
Protein	Lys			Glu/Asp			Asn/Lys		
Pop.a1	A	A	A	G	A	A	A	A	C
Pop.a2	·	·	·	·	·	·	·	·	A
Pop.a3	·	·	·	·	·	·	·	·	A
Pop.a4	·	·	·	·	·	·	·	·	A
Pop.b1	·	·	G	·	·	C	·	·	A
Pop.b2	·	·	G	·	·	C	·	·	A
Pop.b3	·	·	G	·	·	C	·	·	A
Pop.b4	·	·	G	·	·	T	·	·	A
Pop.c1	·	·	G	·	·	C	·	·	·
Pop.c2	·	·	G	·	·	C	·	·	·
Pop.c3	·	·	G	·	·	C	·	·	·
Pop.d1	·	·	G	·	·	C	·	·	A
Pop.d2	·	·	G	·	·	C	·	·	A
Pop.d3	·	·	G	·	·	C	·	·	A
Pop.d4	·	·	G	·	·	T	·	·	A

Note:
a: population-specific site
b: population-specific *Ka* site
c: non-perfect population-specific *Ka* site

D

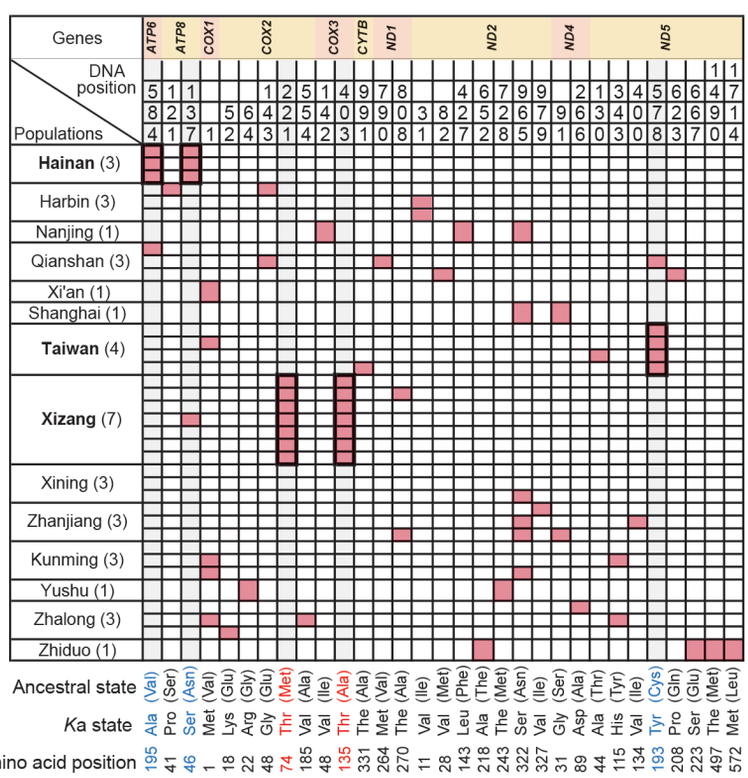

Figure 3 Evolutionary patterns of mitochondrial genes across tree sparrow populations

A: Average number of substitutions (per individual per site) in each population for the 13 protein-coding genes compared to reconstructed ancestral sequences. B: Average number of substitutions (per individual) in rRNAs and tRNAs. Only genes with variable sites are shown. C: Description of population-specific sites. D: K_a (non-synonymous substitution) sites in each population. Perfect (red) and non-perfect (blue) population-specific K_a sites are indicated for Hainan, Taiwan, and Xizang populations. Sample sizes are shown next to each population.

hydrogen bonding between 195Val and 198Phe in *ATP6* (Figure 4B) or the elongation of the bond between 193Tyr and 190Trp in *ND5* (Supplementary Figure S8A). The substitution in *ATP8* (aa46: Asn→Ser; Hainan), located within an intrinsically disordered region, was not predicted to affect overall protein structure (Supplementary Figure S8B).

Impact of mutations on tRNAs: Population-specific mutations in tRNAs, particularly in $tRNA^{Asp}$, were predicted to exert structural and functional effects. In the Hainan population, the insertion of a U at site 18 in $tRNA^{Phe}$ expanded the D loop and shortened the D arm (Supplementary Figure S9A), while a G-to-A substitution at site 29 in $tRNA^{Cys}$ enlarged subloops on the T arm and anticodon arm (Supplementary Figure S9B). A U-to-C substitution at site 5 in $tRNA^{Asp}$ disrupted base pairing in the acceptor stem (Supplementary Figure S9C), increasing steric hindrance and

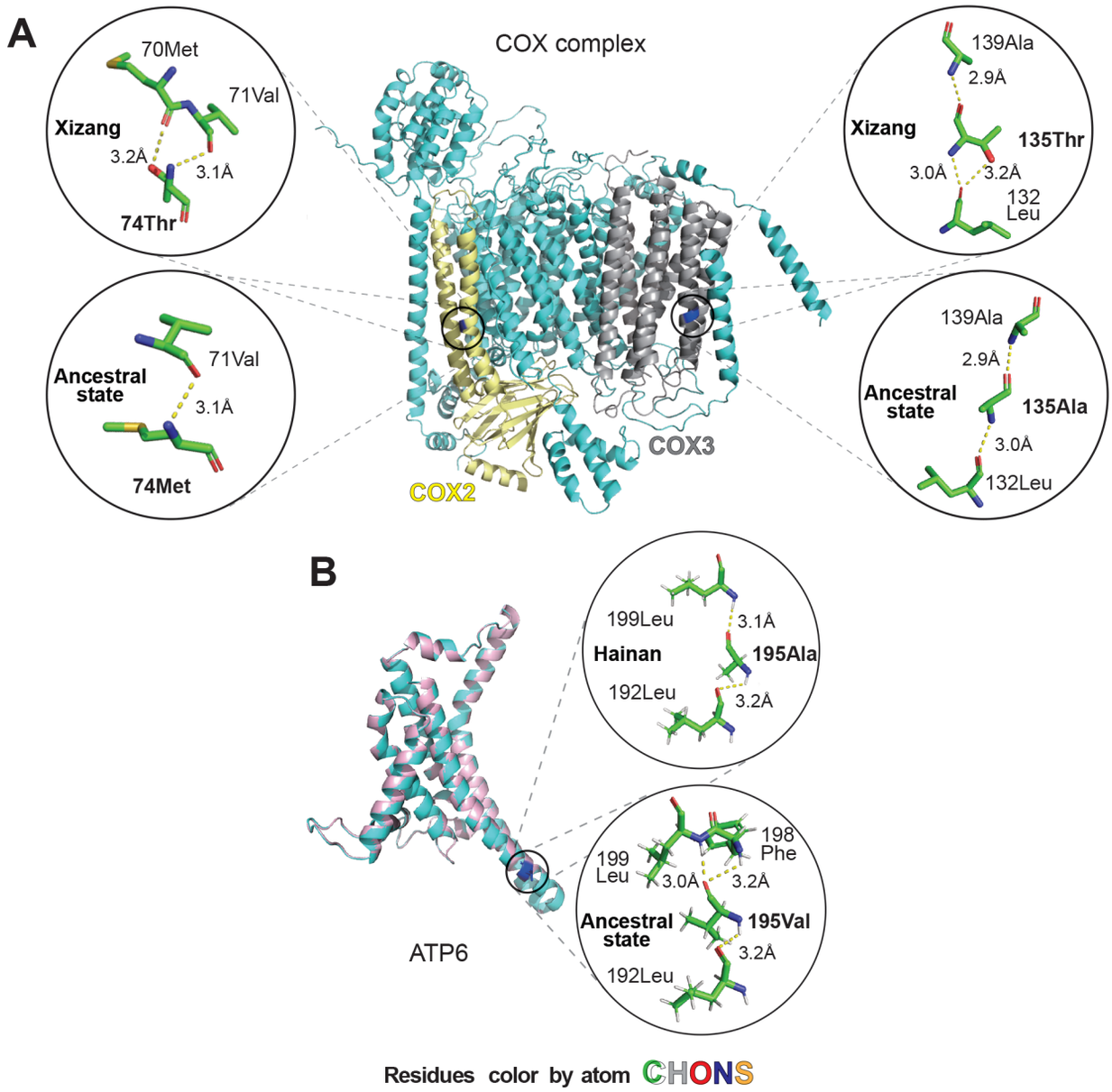

Figure 4 Prediction of protein structures in COX complex and ATP6

A: Structural variations in COX complex at the 74th amino acid (aa) position of COX2 (Thr) and 135th aa position of COX3 (Thr) in the Xizang population compared to the ancestral states (74Met and 135Ala, respectively). Change in COX2 forms an additional 3.2 Å hydrogen bond connecting 74Thr to 70Met; change in COX3 forms an extra 3.2 Å hydrogen bond connecting 135Thr to 132Leu. B: ATP6 structural variation at the 195th aa site in the Hainan population (Ala) compared to the ancestral sequence (Val). 195Ala loses a 3.2 Å bond with 198Phe compared to the ancestral state.

reducing electrostatic potential along the major groove (Figure 5A), thereby likely impairing tRNA recognition and altering functionality (see Discussion). In contrast, the Xizang population carried an A-to-G substitution at site 35 in tRNA^{Asp}, forming a G-U wobble pair (Figures 5B, C; Supplementary Figure S9D) predicted to enhance electrostatic potential and bond flexibility (McClain, 2006).

DISCUSSION

Understanding the drivers of genetic divergence across populations remains fundamental in evolutionary biology. Although species often diverge through well-characterized patterns such as allopatric or ecological speciation (Coyne & Orr, 2004), distinct populations may accumulate unexpected genetic differences due to geographic isolation, demographic shifts, or region-specific selective pressures (e.g., Funk et al., 2012; Hewitt, 2000). The present study integrated mitochondrial and nuclear data from Eurasian tree sparrows to elucidate the extent and origins of population-level genetic differentiation. Analyses of mitogenomes and population-specific substitutions revealed that both geographic isolation and local environmental pressures contribute to shaping genetic structure across populations.

Mitochondrial divergence shaped by geographic and environmental context

Sampling across 36 locations spanning the full ecological and geographic breadth of China yielded the most comprehensive mitogenomic dataset for Eurasian tree sparrows to date (Figure 1). Although generally considered resident birds with constrained dispersal over small ranges (Wang et al., 2020),

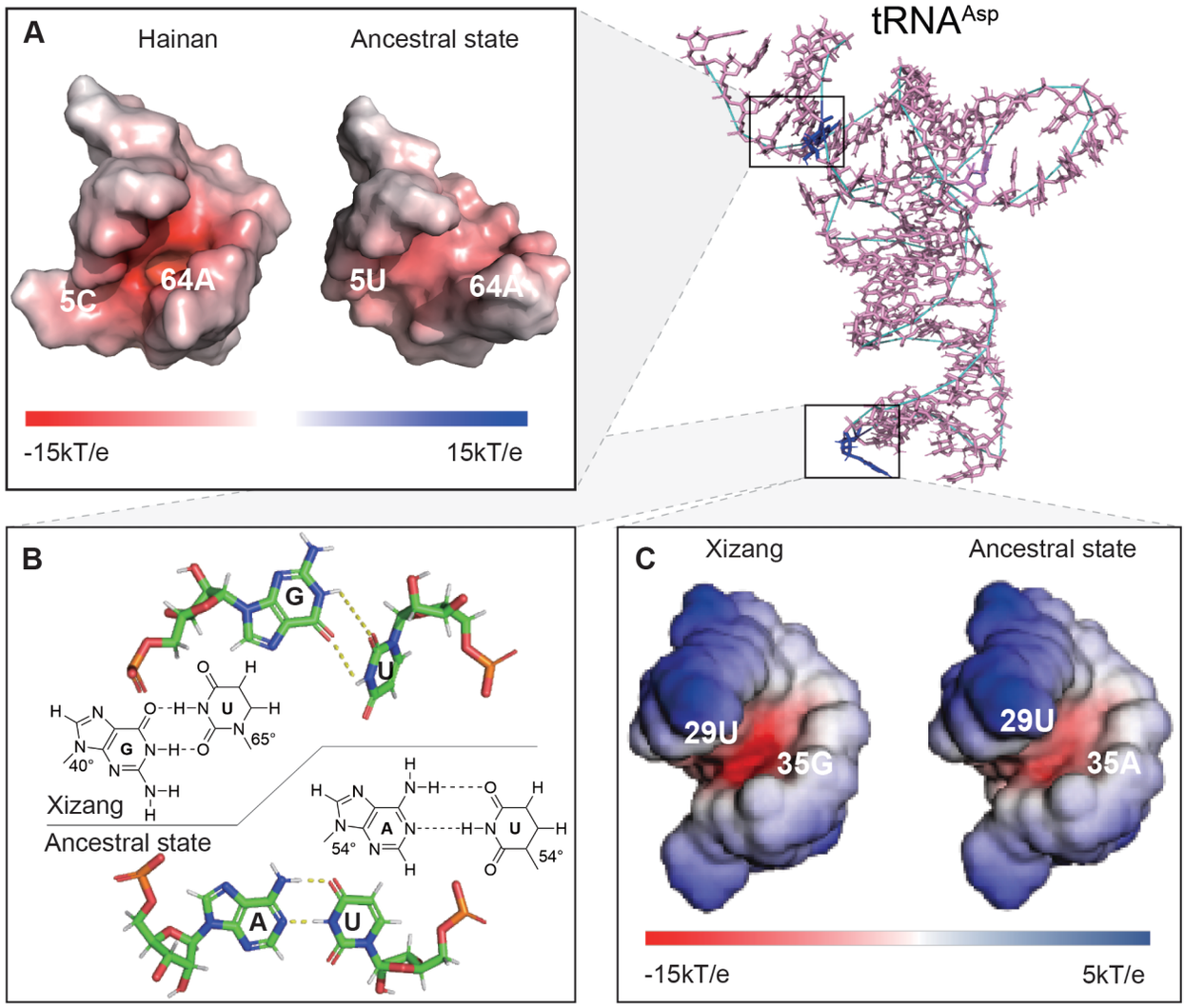

Figure 5 Structural variations of tRNA^{Asp}

A: Hainan population exhibits a U-to-C mutation at site 5, resulting in a 5C-64A pair. This creates greater steric hindrance and reduces electric potential (dark red) in the major groove. B: Xizang population exhibits a population-specific A-to-G change at site 35, forming a G-U Crick wobble pair. C: G-U pair reduces the electrostatic potential (darker red) and facilitates adjustment of the third codon position to accommodate nucleotide binding, thereby enhancing protein synthesis efficiency.

limited but non-negligible gene flow across mainland populations appears plausible, particularly given the partial migration observed in northern latitudes (Barlow et al., 2020). Our results indicated that mitochondrial divergence among most mainland populations was limited, but significant mitogenomic differentiation was observed in geographically isolated regions such as Hainan, Xizang, and Taiwan, as reflected by their elevated F_{ST} values (Table 2), distinct haplotype assemblages, and well-resolved phylogenetic clades (Figure 2). The lack of IBD patterns in the MT2 dataset also suggested that spatial distance alone does not fully account for the observed mitogenomic structure. Instead, a combination of geographic barriers and environmental gradients—supported in part by significant patterns of isolation by environment—likely underlies the divergent mitochondrial lineages detected.

The Xizang population from Dangxiong, Lhasa, occupies a high-altitude environment exceeding 4 000 m a.s.l. on the southern Qinghai-Xizang Plateau. This region acts as a geographic “island”, separated from the mainland by extreme environmental conditions, including hypoxia and pronounced temperature fluctuations (Che et al., 2014; Yao et al., 2000). These stressors impose strong selective pressures on mitochondrial function, favoring mutations that enhance oxidative phosphorylation efficiency (Li et al., 2018). Distinct mitogenomic signatures were detected in the Xizang population (Figure 2), including unique K_a substitutions in *COX2* and *COX3* (Supplementary Table S8), consistent with localized adaptation. Despite occupying similar high-altitude environments and belonging to the same subspecies (*Passer montanus tibetanus*) (Zheng, 2023), tree sparrows from southern Qinghai exhibited relatively limited mitogenomic differentiation compared to lowland populations (Figure 2). These individuals were sampled from Zhiduo and Yushu, regions situated near the plateau margin with direct connectivity to adjacent lowlands. This geographic continuity likely facilitates ongoing gene flow that mitigates mitochondrial divergence (López-Goldar & Agrawal, 2021). In contrast, southern Xizang populations are geographically isolated by extremely high mountain ranges—including the Tanggula, Nyenchen Tanglha, and Himalayas—that act as substantial barriers to dispersal. Reduced connectivity in these areas may

restrict gene flow and amplify local adaptation under migration-selection dynamics (Cheviron & Brumfield, 2009).

Genetic drift and demographic dynamics likely contributed to the emergence of population-specific mutations in Xizang, as evidenced by limited within-population divergence and the presence of shared haplotypes across individuals (Figure 2A). Only two individuals from southern Qinghai were available, highlighting a potential sampling limitation. Interestingly, these individuals displayed distinct genetic profiles and clustered with separate lowland clades rather than the high-altitude Xizang group (Figure 2). Expanded sampling across the southern plateau may help clarify the extent of divergence and disentangle the relative influence of geographic isolation and gene flow.

Both Hainan and Taiwan represent continental island systems exhibiting distinctive mitogenomic signatures (Figures 1, 2). Geographic isolation likely played a central role in shaping the evolutionary trajectories of these populations (Avise, 2000; Zink & Barrowclough, 2008), albeit through divergent mechanisms. The Hainan population formed a deeply divergent mitogenomic lineage (Figure 2) relative to all other sampled populations in China, carrying unique mutations across multiple PCGs and tRNAs (Supplementary Table S8). This pattern may reflect a history of long-term isolation and habitat fragmentation (Li et al., 2006), consistent with expectations for island populations experiencing reduced gene flow and smaller effective population sizes (*N*e), conditions that intensify the effects of genetic drift (Grant & Grant, 2002; Lamichhaney et al., 2018). Tree sparrows in Hainan are currently classified within *Passer montanus malaccensis* (Figure 1), a subspecies distributed across central Myanmar, Malaya, Vietnam, and western Indonesia (Clements et al., 2024). This broader biogeographic range suggests possible historical connectivity between Hainan population and Southeast Asia. Our molecular dating estimates placed the diversification of the Hainan population at approximately 0.024 Ma, coinciding with the final land bridge between Hainan and the Indochina Peninsula during the LGM (ca. 0.026 Ma, Clark et al., 2009). This temporal concordance supports a scenario of historical connectivity followed by isolation, which may have driven the observed genetic distinctiveness of the Hainan population. Additional sampling across Southeast Asia may help reconstruct the divergence history and test for shared ancestry across the broader range.

Taiwan Island experienced a geological history analogous to that of Hainan, with intermittent connection to the mainland during glacial periods, such as the LGM, and sharing the same taxonomic subspecies with adjacent continental populations. Despite this shared ancestry, individuals sampled from Taiwan exhibited distinct mitochondrial haplotypes relative to mainland populations, although the differentiation was less pronounced than that observed in Hainan and Xizang (Figure 2). The reduced number of PSSs in Taiwan may reflect greater historical gene flow—potentially mediated by repeated land connections—or a weaker role of ecological isolation in driving divergence. Comparable patterns of reduced divergence under sustained mainland connectivity have been documented in other island bird systems (e.g., Ballard & Whitlock, 2004).

Numerous non-overlapping population-specific K_s substitutions were detected across mitogenomic genes, particularly in Hainan and Xizang (Supplementary Table S8), underscoring the combined influence of geographic isolation and genetic drift in promoting lineage-specific fixation events (Excoffier et al., 2009).

In contrast, nuclear markers revealed no clear population structure in either the multilocus genetic network or phylogenetic reconstructions (Supplementary Figures S3, S4). Although isothermality (Bio3) and elevation exerted potential influence, nuclear divergence did not correlate with patterns of IBD or IBE (Supplementary Table S6). These results suggest that historical gene flow may have sustained nuclear connectivity across populations, thereby masking clear signals of local differentiation. Alternatively, the absence of structure may reflect insufficient resolution in the available nuclear dataset, as broad single-nucleotide polymorphism (SNP)-based datasets often detect finer-scale population structure than mtDNA (e.g., Toews & Brelsford, 2012). Nevertheless, even large-scale nuclear genomic analyses have revealed only shallow divergence between highland and lowland tree sparrow populations, despite substantial phenotypic differences (Qu et al., 2020). Thus, the pronounced mitochondrial divergence observed in certain populations may also reflect the higher sensitivity of mtDNA to demographic and evolutionary processes, potentially linked to its maternal inheritance and smaller *N*e (Ballard & Whitlock, 2004).

Mitogenomic variation and signatures of population adaptation

Mitogenomic variation contributes to population divergence and may underlie adaptive processes (Ruiz-Pesini et al., 2004; Tomasco & Lessa, 2011), particularly in extreme environments such as high-altitude habitats. Unique mutations in both protein-coding and tRNA genes were identified in geographically isolated tree sparrow populations. Structural modeling indicated that these variants could alter protein stability and function, consistent with earlier findings linking mtDNA mutations to changes in oxidative phosphorylation efficiency (da Fonseca et al., 2008; Scott et al., 2011).

Potential high-altitude adaptation: In the genetically divergent Xizang population, multiple population-specific K_a sites were identified in *COX2* and *COX3* (Figure 3), with several sites showing putative evidence of positive selection (Supplementary Tables S9, S10; $P<0.05$ or BEB>0.5). Structural modeling suggested that these substitutions may enhance protein rigidity by introducing additional hydrogen bonds at the mutation sites (Sljoka, 2022; Figure 4A). Enhanced rigidity within mitochondrial proteins may improve thermogenic efficiency in cold environments, as mitochondria serve as primary sites of heat production (Midtgård, 1989; Zheng et al., 2014). Furthermore, a specific Ala substitution located within the v-cleft of COX3 may facilitate oxygen channeling into the catalytic core of the COX complex, potentially enhancing aerobic metabolism under hypoxic conditions (Leeuwis & Gamperl, 2022). Similar mechanisms have been reported in high-altitude taxa such as the bar-headed goose (*Anser indicus*), where mutations in *COX* increase enzyme kinetics and oxygen transport capacity, enabling efficient energy production and sustained flight under hypoxic conditions (Scott et al., 2011).

In addition to PCG mutations, a population-specific $tRNA^{Asp}$ mutation was also detected in the Xizang population (Supplementary Table S8). This A-to-G substitution at position 35 in the anticodon arm generated a G-U wobble pair (Figure 5B, C), predicted to enhance flexibility of the ribose-phosphate backbone (Varani & McClain, 2000). Increased

structural flexibility may facilitate improved decoding dynamics and translational efficiency under variable environmental pressures (McClain, 2006; Varani & McClain, 2000). Given the central role of tRNAs in mitochondrial protein synthesis, such mutations may exert a more profound influence on mitochondrial function than isolated PCG mutations (Ottenburghs et al., 2021; Schon et al., 2012), potentially driving functional differentiation across populations.

Collectively, mitochondrial mutations in the Xizang population, including substitutions in *COX* and tRNA genes, may represent candidate adaptations to cold and hypoxic stress at high altitudes. However, experimental validation is required to determine the physiological relevance of these substitutions and their mechanistic roles in thermogenesis and oxygen utilization.

Putative mitochondrial adaptations in tropical and subtropical island populations: Island populations occupying thermally stable yet ecologically distinct environments may undergo divergent selective and demographic processes affecting mitochondrial function. Hainan experiences a persistently humid tropical climate, with annual mean temperatures between 23–25°C and relative humidity exceeding 80%, whereas Taiwan features a subtropical, mountainous landscape with mean temperatures ranging from 16–25°C. These environmental conditions may impose distinct metabolic demands, potentially shaping mitogenomic evolution.

Within the Hainan population, candidate adaptive substitutions were identified in *ATP6* (Figure 4B), while the Taiwan population harbored non-perfect population-specific variants in *ND5* (Supplementary Table S9 and Figure S8). Structural modeling indicated that these mutations may enhance molecular flexibility by reducing local hydrogen bonding or increasing bond lengths (Dereka et al., 2021; Fersht et al., 1985), a shift potentially favoring mitochondrial efficiency under environmental fluctuation (e.g., Dhar et al., 2021). However, given the limitations of homology-based modeling and lack of experimental validation within the scope of the current study, the functional interpretation of these mutations remains tentative. Moreover, although IBE analyses identified correlations between mitogenomic divergence and environmental factors—with elevation showing some effect (Supplementary Table S6)—pinpointing the specific environmental pressures driving this divergence remains challenging given the complex interplay of environmental variables across locations.

Relaxed purifying selection was detected at *CYTB* in the Taiwan population (Supplementary Table S11), suggesting a reduction in selective constraint that may contribute to mitochondrial divergence. Such relaxation—defined by diminished efficacy of natural selection—has been linked to the evolutionary loss of complex traits, such as flight in insects and birds (Li et al., 2018; Shen et al., 2009), vision in cave-dwelling fish (Darwin, 1895), and pseudogenization of the *SWS1* gene in cave-roosting and echolocating bats (Wertheim et al., 2015). Relaxed selection can also permit the accumulation of neutral or slightly deleterious mutations, contributing to the gradual decay of nonfunctional traits and population divergence over time (Lahti et al., 2009), as possibly reflected by the mitogenomic divergence between the Hainan and Taiwan populations (Figure 2).

Population specific tRNA variants in the Hainan population further supported its distinctiveness, with predicted structural modifications including loop enlargement (Supplementary Figure S9A, B) and disruption of pairing interactions (Figure 5A; Supplementary Figure S9C). Although many tRNA mutations remain functionally "tolerated" (Schon et al., 2012), others have been linked to pathophysiology (Goodarzi et al., 2016; Jones et al., 2008). In this case, the population-specific tRNA changes in the Hainan population may reflect functional relaxation. However, in small populations (e.g., island populations), diminished *N*e weakens purifying selection, enabling the persistence of neutral or mildly deleterious variants (Grant & Grant, 2002; Ohta, 1973; Romiguier et al., 2014; Woolfit & Bromham, 2005). Thus, the tRNA divergence in Hainan could also arise from genetic drift-driven fixation of variants rather than adaptive relaxation.

Demography of tree sparrows in China

The demographic history of Eurasian tree sparrows across China reflects a complex interplay between ecological opportunity and anthropogenic influence. As a synanthropic species closely tied to the expansion of agriculture and permanent human habitation (Barlow et al., 2020), tree sparrows have long been presumed to have colonized the Qinghai-Xizang Plateau approximately 2 600 years ago, coinciding with the introduction of cold-adapted crops such as wheat and barley (Chen et al., 2015; Lu, 2016). In the present study, the mitogenomic analyses (MT15) revealed a markedly deeper evolutionary history. Notably, the crown lineage of the tree sparrow was estimated to have originated 0.2 Ma, with diversification within the Xizang population beginning approximately 22 000 years ago (Supplementary Figure S6), predating the onset of permanent human settlement and more closely aligning with archaeological evidence of early human presence on the plateau (Aldenderfer, 2011; Brantingham et al., 2007).

The discrepancy between current and previous time estimates likely stems from methodological and sampling differences. Mitogenomes, while informative, may not fully capture the demographic complexity detectable with genome-wide nuclear data. Moreover, mtDNA-based time estimates are sensitive to substitution rate assumptions and may predate actual population splits due to incomplete lineage sorting (ILS; Ballard & Whitlock, 2004). Nonetheless, the smaller N_e of mtDNA may reduce the extent of this confounding. The shallow divergence inferred by Qu et al. (2020) may also reflect sampling limitations. Their highland samples were collected from Heimahe in northeastern Qinghai, a region located outside the core region of the Qinghai-Xizang Plateau. In the current study, samples from Xining, which is geographically close to Heimahe, clustered with lowland lineages in mitochondrial phylogenies (Figure 2), implying limited divergence in this region. The absence of individuals from the southern plateau in earlier studies may have masked deeper population structure, leading to an underestimation of highland-lowland differentiation. Notably, archaeological and genetic evidence supports human presence in the high-altitude interior of the plateau as early as 30 000 years ago (Qi et al., 2013; Zhang et al., 2018), indicating that tree sparrow colonization of these environments may have occurred much earlier than previously inferred.

Population dynamics inferred from Bayesian Skyline Plot (BSP) analyses showed only minor fluctuations in the N_e of tree sparrows over time (Supplementary Figure S7), consistent with long-term demographic stability. While BSP is

effective for reconstructing extended historical dynamics, it lacks the sensitivity to resolve recent population changes (Heled & Drummond, 2008). Future studies incorporating high-density SNP datasets with high-resolution methods, such as genetic optimization for N_e estimation (GONE; Santiago et al., 2020) may better capture recent demographic shifts, including signals potentially associated with historical ecosystem disturbances, such as the late-1950s "Smash Sparrows Campaign" in China (Chen, 2009).

CONCLUSIONS AND IMPLICATIONS

Mitogenomic analyses revealed pronounced regional differentiation in tree sparrows from geographically isolated regions, including southern Xizang on the Qinghai-Xizang Plateau and the continental islands of Hainan and Taiwan. These patterns emphasize the critical role of mitogenomic analyses in resolving fine-scale population structure. Additionally, population-specific mutations in mitogenomes may reflect responses to localized environmental pressures. For instance, Xizang-specific substitutions in COX2 and COX3 may stabilize protein conformation through enhanced hydrogen bonding, while structural variations in ATP6 and $tRNA^{Asp}$ in the Hainan population may potentially influence molecular function. Nonetheless, the limited power of selection analyses and limitations in sampling leave open the possibility that these patterns reflect stochastic processes such as genetic drift.

While previous research has predominantly focused on mitogenomic adaptation in extreme environments, such as high-altitude or polar regions (Scott et al., 2009; Xu et al., 2005), the current findings point to a broader role of mitogenomes in mediating responses to both geographic isolation and diverse ecological contexts, providing new insights into the potential functional consequences of mitogenomic variation. Although population-specific mutations were identified and their potential selective significance was inferred, further validation is required to confirm their adaptive significance. For instance, protein structure modeling only offers preliminary insights into the structural impacts of mitogenomic variation. To validate the functional consequences of these changes—particularly their effects on mitochondrial efficiency and protein function—comprehensive follow-up analyses, such as biochemical and physiological experiments, will be essential. Additionally, integrating genome-wide nuclear analyses with demographic modeling will yield a more comprehensive understanding of the evolutionary mechanisms shaping the divergence and adaptation of tree sparrow populations.

DATA AVAILABILITY

All sequencing data generated in this study (including 829 gene segments and 39 whole mitogenomes) were deposited in GenBank (accession numbers PQ767157–PQ767985 and PQ783074–PQ783112), GenBase at the National Genomics Data Center (GB0006596, GB0006595, GB0006594, GB0006593, and GB0006578), and the Science Data Bank (SDB, Data DOI: 10.57760/sciencedb.j00139.00252).

SUPPLEMENTARY DATA

Supplementary data, including figures, tables, alignments, and phylogenetic tree files, can be found online.

COMPETING INTERESTS

The authors declare that they have no competing interests.

AUTHORS' CONTRIBUTIONS

B.L. and N.W. designed the study. W.L., L.W.W., L.Y., Y.L.L., H.T.W., and B.L. collected the samples. B.L. and N.W. conducted the lab work. W.X. performed the mitogenomic sequencing. Q.L. and X.J.Z. provided suggestions on mitogenome assembly, and B.L. performed the assembly. C.B.S. and N.W. performed data analysis. N.W., C.B.S., H.M., and S.L. reviewed the analyses and first draft of the manuscript. All authors read and approved the final version of the manuscript.

ACKNOWLEDGMENTS

We sincerely thank Professor Jian Lei and Dr. Kai Wang from Sichuan University for their guidance on protein structure simulation and interpretation. We also thank Rebecca Kimball and Edward Braun from the University of Florida for their constructive feedback on an earlier version of this paper. We offer special thanks to Dr. Tong-Jian Liu from the South China Botanical Garden, Chinese Academy of Sciences, for guidance on using Geneious Prime. Finally, we extend our gratitude to everyone who assisted with tree sparrow sample collection.

REFERENCES

Aldenderfer M. 2011. Peopling the Tibetan plateau: insights from archaeology. *High Altitude Medicine & Biology*, **12**(2): 141–147.

Álvarez-Carretero S, Kapli P, Yang ZH. 2023. Beginner's guide on the use of PAML to detect positive selection. *Molecular Biology and Evolution*, **40**(4): msad041.

Arcones A, Ponti R, Vieites DR. 2021. Mitochondrial substitution rates estimation for divergence time analyses in modern birds based on full mitochondrial genomes. *Ibis*, **163**(4): 1463–1471.

Avise J C. 2000. Phylogeography: the History and Formation of Species. London: Harvard University Press.

Balcão VM, Vila MMDC. 2015. Structural and functional stabilization of protein entities: *state-of-the-art*. *Advanced Drug Delivery Reviews*, **93**: 25–41.

Ballard JWO, Whitlock MC. 2004. The incomplete natural history of mitochondria. *Molecular Ecology*, **13**(4): 729–744.

Balloux F, Handley LJL, Jombart T, et al. 2009. Climate shaped the worldwide distribution of human mitochondrial DNA sequence variation. *Proceedings of the Royal Society B: Biological Sciences*, **276**(1672): 3447–3455.

Barlow JC, Leckie SN, Pyle P, et al. 2020. Eurasian tree sparrow (*Passer montanus*), version 1.0. *In*: Billerman S M. Birds of the World. Ithaca: Cornell Lab of Ornithology.

Bouckaert R, Vaughan TG, Barido-Sottani J, et al. 2019. BEAST 2.5: an advanced software platform for Bayesian evolutionary analysis. *PLoS Computational Biology*, **15**(4): e1006650.

Brantingham PJ, Gao X, Olsen JW, et al. 2007. A short chronology for the peopling of the Tibetan Plateau. *Developments in Quaternary Sciences*, **9**: 129–150.

Bryant D, Moulton V. 2004. Neighbor-Net: an agglomerative method for the construction of phylogenetic networks. *Molecular Biology and Evolution*, **21**(2): 255–265.

Cerasoli F, D'Alessandro P, Biondi M. 2022. Worldclim 2.1 versus Worldclim 1.4: climatic niche and grid resolution affect between‐version mismatches in habitat suitability models predictions across Europe. *Ecology and Evolution*, **12**(2): e8430.

Che ML, Chen BZ, Innes JL, et al. 2014. Spatial and temporal variations in the end date of the vegetation growing season throughout the Qinghai–Tibetan Plateau from 1982 to 2011. *Agricultural and Forest Meteorology*, **189-190**: 81–90.

Chen Y. 2009. Cold War competition and food production in China, 1957–1962. *Agricultural History*, **83**(1): 51–78.

Chen FH, Dong GH, Zhang DJ, et al. 2015. Agriculture facilitated permanent human occupation of the Tibetan Plateau after 3600 B. P. *Science*, **347**(6219): 248–250.

Cheviron ZA, Brumfield RT. 2009. Migration-selection balance and local adaptation of mitochondrial haplotypes in Rufous-collared sparrows (*Zonotrichia capensis*) along an elevational gradient. *Evolution*, **63**(6): 1593–1605.

Clark PU, Dyke AS, Shakun JD, et al. 2009. The last glacial maximum. *Science*, **325**(5941): 710–714.

Clements JF, Rasmussen PC, Schulenberg TS, et al. 2024. The eBird/Clements checklist of Birds of the World: v2024.

Coyne JA, Orr HA. 2004. Speciation. Sunderland: Sinauer Associates, Inc. , 272–292.

da Fonseca RR, Johnson WE, O'brien SJ, et al. 2008. The adaptive evolution of the mammalian mitochondrial genome. *BMC Genomics*, **9**: 119.

Darriba D, Taboada GL, Doallo R, et al. 2012. jModelTest 2: more models, new heuristics and parallel computing. *Nature Methods*, **9**(8): 772.

Darwin CR. 1895. On the Origin of Species by Means of Natural Selection, or the Preservation of Favoured Races in the Struggle for Life. London: John Murray.

Delano WL. 2002. PyMOL: an open-source molecular graphics tool. *CCP4 Newsl. Protein Crystallogr*, **40**(1): 82–92.

Dereka B, Yu Q, Lewis NHC, et al. 2021. Crossover from hydrogen to chemical bonding. *Science*, **371**(6525): 160–164.

Dhar D, Dey D, Basu S, et al. 2021. Insight into the adaptive evolution of mitochondrial genomes in intertidal chitons. *Journal of Molluscan Studies*, **87**(2): eyab018.

Ding BY, Zhao YL, Sun YF, et al. 2021. Coping with extremes: lowered myocardial phosphofructokinase activities and glucose content but increased fatty acids content in highland Eurasian Tree Sparrows. *Avian Research*, **12**: 44.

Evans R, O'Neill M, Pritzel A, et al. 2021. Protein complex prediction with AlphaFold-Multimer. *Biorxiv*, doi: https://doi.org/10.1101/2021.10.04.463034.

Excoffier L, Foll M, Petit RJ. 2009. Genetic consequences of range expansions. *Annual Review of Ecology, Evolution, and Systematics*, **40**: 481–501.

Excoffier L, Lischer HEL. 2010. Arlequin suite ver 3.5: a new series of programs to perform population genetics analyses under Linux and Windows. *Molecular Ecology Resources*, **10**(3): 564–567.

Fersht AR, Wilkinson AJ, Carter P, et al. 1985. Fine structure-activity analysis of mutations at position 51 of tyrosyl-tRNA synthetase. *Biochemistry*, **24**(21): 5858–5861.

Fontanillas P, Dépraz A, Giorgi MS, et al. 2005. Nonshivering thermogenesis capacity associated to mitochondrial DNA haplotypes and gender in the greater white‐toothed shrew, *Crocidura russula*. *Molecular Ecology*, **14**(2): 661–670.

Fu YX, Li WH. 1993. Statistical tests of neutrality of mutations. *Genetics*, **133**(3): 693–709.

Funk WC, McKay JK, Hohenlohe PA, et al. 2012. Harnessing genomics for delineating conservation units. *Trends in Ecology & Evolution*, **27**(9): 489–496.

Goodarzi H, Nguyen HCB, Zhang S, et al. 2016. Modulated expression of specific tRNAs drives gene expression and cancer progression. *Cell*, **165**(6): 1416–1427.

Grant PR, Grant BR. 2002. Unpredictable evolution in a 30-year study of Darwin's finches. *Science*, **296**(5568): 707–711.

Heled J, Drummond AJ. 2008. Bayesian inference of population size history from multiple loci. *BMC Evolutionary Biology*, **8**(1): 289.

Hewitt G. 2000. The genetic legacy of the Quaternary ice ages. *Nature*, **405**(6789): 907–913.

Hudson RR, Slatkin M, Maddison WP. 1992. Estimation of levels of gene flow from DNA sequence data. *Genetics*, **132**(2): 583–589.

Huson DH. 1998. SplitsTree: analyzing and visualizing evolutionary data. *Bioinformatics*, **14**(1): 68–73.

Jones CN, Jones CI, Graham WD, et al. 2008. A disease-causing point mutation in human mitochondrial $tRNA^{Met}$ results in tRNA misfolding leading to defects in translational initiation and elongation. *Journal of Biological Chemistry*, **283**(49): 34445–34456.

Jumper J, Evans R, Pritzel A, et al. 2021. Highly accurate protein structure prediction with AlphaFold. *Nature*, **596**(7873): 583–589.

Jurrus E, Engel D, Star K, et al. 2018. Improvements to the APBS biomolecular solvation software suite. *Protein Science*, **27**(1): 112–128.

Kang LL, Zheng HX, Chen F, et al. 2013. mtDNA lineage expansions in Sherpa population suggest adaptive evolution in Tibetan highlands. *Molecular Biology and Evolution*, **30**(12): 2579–2587.

Kosakovsky Pond SL, Poon AFY, Velazquez R, et al. 2020. HyPhy 2.5—a customizable platform for evolutionary hypothesis testing using phylogenies. *Molecular Biology and Evolution*, **37**(1): 295–299.

Kozlov AM, Darriba D, Flouri T, et al. 2019. RAxML-NG: a fast, scalable and user-friendly tool for maximum likelihood phylogenetic inference. *Bioinformatics*, **35**(21): 4453–4455.

Lahti DC, Johnson NA, Ajie BC, et al. 2009. Relaxed selection in the wild. *Trends in Ecology & Evolution*, **24**(9): 487–496.

Lamichhaney S, Han F, Webster MT, et al. 2018. Rapid hybrid speciation in Darwin's finches. *Science*, **359**(6372): 224–228.

Leeuwis RHJ, Gamperl AK. 2022. Adaptations and plastic phenotypic responses of marine animals to the environmental challenges of the high intertidal zone. Leeuwis & Gamperl 2022 Oceanography and Marine Biology: An Annual Review, 60: 625–679.

Leigh JW, Bryant D. 2015. POPART: full-feature software for haplotype network construction. *Methods in Ecology and Evolution*, **6**(9): 1110–1116.

Li SB, Gao H, Liu JL, et al. 2022. Life history variation between two Eurasian tree sparrow *Passer montanus* populations at different altitudes. *Animal Biology*, **72**(4): 385–394.

Li SH, Li JW, Han LX, et al. 2006. Species delimitation in the Hwamei *Garrulax canorus*. *Ibis*, **148**(4): 698–706.

Li XD, Jiang GF, Yan LY, et al. 2018. Positive selection drove the adaptation of mitochondrial genes to the demands of flight and high-altitude environments in grasshoppers. *Frontiers in Genetics*, **9**: 605.

Liang B, Wang N, Li N, et al. 2018. Comparative genomics reveals a burst of homoplasy-free *numt* insertions. *Molecular Biology and Evolution*, **35**(8): 2060–2064.

López-Goldar X, Agrawal AA. 2021. Ecological interactions, environmental gradients, and gene flow in local adaptation. *Trends in Plant Science*, **26**(8): 796–809.

Lu HL. 2016. Colonization of the Tibetan Plateau, permanent settlement, and the spread of agriculture: reflection on current debates on the prehistoric archeology of the Tibetan Plateau. *Archaeological Research in Asia*, **5**: 12–15.

McClain WH. 2006. Surprising contribution to aminoacylation and translation of non-Watson-Crick pairs in tRNA. *Proceedings of the National Academy of Sciences of the United States of America*, **103**(12): 4570–4575.

Midtgård U. 1989. Circulatory adaptations to cold in birds. *In*: Bech C, Reinertsen RE. Physiology of Cold Adaptation in Birds. Boston: Springer, 211–222.

Mirdita M, Steinegger M, Söding J. 2019. MMseqs2 desktop and local web server app for fast, interactive sequence searches. *Bioinformatics*, **35**(16): 2856–2858.

Monsanto DM, Main DC, Janion-Scheepers C, et al. 2022. Mitogenome selection in the evolution of key ecological strategies in the ancient hexapod class Collembola. *Scientific Reports*, **12**(1): 14810.

Morales HE, Pavlova A, Amos N, et al. 2018. Concordant divergence of mitogenomes and a mitonuclear gene cluster in bird lineages inhabiting different climates. *Nature Ecology & Evolution*, **2**(8): 1258–1267.

Morales HE, Pavlova A, Joseph L, et al. 2015. Positive and purifying selection in mitochondrial genomes of a bird with mitonuclear discordance. *Molecular Ecology*, **24**(11): 2820–2837.

Nielsen R, Yang ZH. 1998. Likelihood models for detecting positively selected amino acid sites and applications to the HIV-1 envelope gene. *Genetics*, **148**(3): 929–936.

Ohta T. 1973. Slightly deleterious mutant substitutions in evolution. *Nature*, **246**(5428): 96–98.

Ottenburghs J, Geng KY, Suh A, et al. 2021. Genome size reduction and transposon activity impact tRNA gene diversity while ensuring translational stability in birds. *Genome Biology and Evolution*, **13**(4): evab016.

Päckert M, Hering J, Belkacem AA, et al. 2021. A revised multilocus phylogeny of Old World sparrows (Aves: Passeridae). *Vertebrate Zoology*, **71**: 353–366.

Phillips SJ, Anderson RP, Schapire RE. 2006. Maximum entropy modeling of species geographic distributions. *Ecological modelling*, **190**(3-4): 231–259.

Powell JR. 1994. Molecular techniques in population genetics: a brief history. *In*: Schierwater B, Streit B, Wagner GP, et al. Molecular Ecology and Evolution: Approaches and Applications. Birkhäuser: Springer, 131–156.

Qi XB, Cui CY, Peng Y, et al. 2013. Genetic evidence of Paleolithic colonization and Neolithic expansion of modern humans on the Tibetan plateau. *Molecular Biology and Evolution*, **30**(8): 1761–1778.

Qu YH, Chen CH, Xiong Y, et al. 2020. Rapid phenotypic evolution with shallow genomic differentiation during early stages of high elevation adaptation in Eurasian Tree Sparrows. *National Science Review*, **7**(1): 113–127.

Rambaut A, Drummond AJ, Xie D, et al. 2018. Posterior summarization in Bayesian phylogenetics using Tracer 1.7. *Systematic Biology*, **67**(5): 901–904.

Roger AJ, Muñoz-Gómez SA, Kamikawa R. 2017. The origin and diversification of mitochondria. *Current Biology*, **27**(21): R1177–R1192.

Romiguier J, Gayral P, Ballenghien M, et al. 2014. Comparative population genomics in animals uncovers the determinants of genetic diversity. *Nature*, **515**(7526): 261–263.

Ramos B, González-Acuña D, Loyola DE, et al. 2018. Landscape genomics: natural selection drives the evolution of mitogenome in penguins. *BMC Genomics*, **19**(1): 53–70.

Ronquist F, Huelsenbeck JP. 2003. MrBayes 3: Bayesian phylogenetic inference under mixed models. *Bioinformatics*, **19**(12): 1572–1574.

Rousset F. 1997. Genetic differentiation and estimation of gene flow from *F*-statistics under isolation by distance. *Genetics*, **145**(4): 1219–1228.

Rozas J, Ferrer-Mata A, Sánchez-Delbarrio JC, et al. 2017. DnaSP 6: DNA sequence polymorphism analysis of large data sets. *Molecular Biology and Evolution*, **34**(12): 3299–3302.

Ruiz-Pesini E, Mishmar D, Brandon M, et al. 2004. Effects of purifying and adaptive selection on regional variation in human mtDNA. *Science*, **303**(5655): 223–226.

Santiago E, Novo I, Pardiñas AF, et al. 2020. Recent demographic history inferred by high-resolution analysis of linkage disequilibrium. *Molecular Biology and Evolution*, **37**(12): 3642–3653.

Sato K, Akiyama M, Sakakibara Y. 2021. RNA secondary structure prediction using deep learning with thermodynamic integration. *Nature Communications*, **12**(1): 941.

Schon EA, Dimauro S, Hirano M. 2012. Human mitochondrial DNA: roles of inherited and somatic mutations. *Nature Reviews Genetics*, **13**(12): 878–890.

Scott GR, Egginton S, Richards JG, et al. 2009. Evolution of muscle phenotype for extreme high altitude flight in the bar-headed goose. *Proceedings of the Royal Society B: Biological Sciences*, **276**(1673): 3645–3653.

Scott GR, Schulte PM, Egginton S, et al. 2011. Molecular evolution of cytochrome c oxidase underlies high-altitude adaptation in the bar-headed goose. *Molecular Biology and Evolution*, **28**(1): 351–363.

Shaffer JP. 1995. Multiple hypothesis testing. *Annual Review of Psychology*, **46**(1): 561–584.

Shen K, Pender CL, Bar-Ziv R, et al. 2022. Mitochondria as cellular and organismal signaling hubs. *Annual Review of Cell and Developmental Biology*, **38**(1): 179–218.

Shen YY, Shi P, Sun YB, et al. 2009. Relaxation of selective constraints on avian mitochondrial DNA following the degeneration of flight ability. *Genome Research*, **19**(10): 1760–1765.

Sljoka A. 2022. Structural and functional analysis of proteins using rigidity theory. *In*: Katoh N, Higashikawa Y, Ito H, et al. Sublinear Computation Paradigm: Algorithmic Revolution in the Big Data Era. Singapore: Springer, 337–367.

Smouse PE, Long JC, Sokal RR. 1986. Multiple regression and correlation extensions of the mantel test of matrix correspondence. *Systematic Biology*, **35**(4): 627–632.

Stamatakis A. 2006. RAxML-VI-HPC: maximum likelihood-based phylogenetic analyses with thousands of taxa and mixed models. *Bioinformatics*, **22**(21): 2688–2690.

Steinegger M, Meier M, Mirdita M, et al. 2019. HH-suite3 for fast remote homology detection and deep protein annotation. *BMC Bioinformatics*, **20**(1): 473.

Stephens M, Smith NJ, Donnelly P. 2001. A new statistical method for haplotype reconstruction from population data. *The American Journal of Human Genetics*, **68**(4): 978–989.

Stewart JB, Chinnery PF. 2015. The dynamics of mitochondrial DNA heteroplasmy: implications for human health and disease. *Nature Reviews Genetics*, **16**(9): 530–542.

Sun YF, Ren ZP, Wu YF, et al. 2016. Flying high: limits to flight performance by sparrows on the Qinghai-Tibet Plateau. *The Journal of Experimental Biology*, **219**(22): 3642–3648.

Tajima F. 1989. Statistical method for testing the neutral mutation hypothesis by DNA polymorphism. *Genetics*, **123**(3): 585–595.

Tamura K, Nei M, Kumar S. 2004. Prospects for inferring very large phylogenies by using the neighbor-joining method. *Proceedings of the National Academy of Sciences of the United States of America*, **101**(30): 11030–11035.

Tamura K, Stecher G, Kumar S. 2021. MEGA11: molecular evolutionary genetics analysis version 11. *Molecular Biology and Evolution*, **38**(7): 3022–3027.

Templeton AR, Crandall KA, Sing CF. 1992. A cladistic analysis of phenotypic associations with haplotypes inferred from restriction endonuclease mapping and DNA sequence data. III. Cladogram estimation. *Genetics*, **132**(2): 619–633.

Toews DPL, Brelsford A. 2012. The biogeography of mitochondrial and nuclear discordance in animals. *Molecular Ecology*, **21**(16): 3907–3930.

Tomasco IH, Lessa EP. 2011. The evolution of mitochondrial genomes in subterranean caviomorph rodents: adaptation against a background of purifying selection. *Molecular Phylogenetics and Evolution*, **61**(1): 64–70.

Varani G, McClain WH. 2000. The G·U wobble base pair. A fundamental building block of RNA structure crucial to RNA function in diverse biological systems. *EMBO Reports*, **1**(1): 18–23.

Vieira AR, de Sousa F, Bilro J, et al. 2024. Mitochondrial genomes of the European sardine (*Sardina pilchardus*) reveal Pliocene diversification, extensive gene flow and pervasive purifying selection. *Scientific Reports*,

14(1): 30977.
Wallace DC. 2015. Mitochondrial DNA variation in human radiation and disease. *Cell*, **163**(1): 33–38.
Wang IJ. 2013. Examining the full effects of landscape heterogeneity on spatial genetic variation: a multiple matrix regression approach for quantifying geographic and ecological isolation. *Evolution*, **67**(12): 3403–3411.
Wang N, Hosner PA, Liang B, et al. 2017. Historical relationships of three enigmatic phasianid genera (Aves: Galliformes) inferred using phylogenomic and mitogenomic data. *Molecular Phylogenetics and Evolution*, **109**: 217–225.
Wang N, Liang B. 2016. Complete mitochondrial genome of a sunbird, *Aethopyga gouldiae* (Aves: Passeriformes), the first representative of Nectariniidae. *Mitochondrial DNA Part A*, **27**(4): 2356–2358.
Wang N, Liang B, Wang JC, et al. 2016. Incipient speciation with gene flow on a continental island: species delimitation of the Hainan Hwamei (*Leucodioptron canorum owstoni*, Passeriformes, Aves). *Molecular Phylogenetics and Evolution*, **102**: 62–73.
Wang Y, Yin Y, Ren ZP, et al. 2020. A comparison of flight energetics and kinematics of migratory Brambling and residential Eurasian Tree Sparrow. *Avian Research*, **11**(1): 25.
Warren DL, Glor RE, Turelli M. 2010. ENMTools: a toolbox for comparative studies of environmental niche models. *Ecography*, **33**(3): 607–611.
Weir BS, Cockerham CC. 1984. Estimating *F*-statistics for the analysis of population structure. *Evolution*, **38**(6): 1358–1370.
Wertheim JO, Murrell B, Smith MD, et al. 2015. RELAX: detecting relaxed selection in a phylogenetic framework. *Molecular Biology and Evolution*, **32**(3): 820–832.
Woolfit M, Bromham L. 2005. Population size and molecular evolution on islands. *Proceedings of the Royal Society B: Biological Sciences*, **272**(1578): 2277–2282.
Xiong Y, Fan LQ, Hao Y, et al. 2020. Physiological and genetic convergence supports hypoxia resistance in high-altitude songbirds. *PLoS Genetics*, **16**(12): e1009270.
Xu SQ, Luosang JB, Hua S, et al. 2007. High altitude adaptation and phylogenetic analysis of Tibetan horse based on the mitochondrial genome. *Journal of Genetics and Genomics*, **34**(8): 720–729.
Xu SQ, Yang YZ, Zhou J, et al. 2005. A mitochondrial genome sequence of the Tibetan antelope (*Pantholops hodgsonii*). *Genomics, Proteomics & Bioinformatics*, **3**(1): 5–17.
Yang Z. 1998. Likelihood ratio tests for detecting positive selection and application to primate lysozyme evolution. *Molecular Biology and Evolution*, **15**(5): 568–573.
Yang Z. 2007. PAML 4: phylogenetic analysis by maximum likelihood. *Molecular Biology and Evolution*, **24**(8): 1586–1591.
Yang ZH, dos Reis M. 2011. Statistical properties of the branch-site test of positive selection. *Molecular Biology and Evolution*, **28**(3): 1217–1228.
Yang ZH, Wong WSW, Nielsen R. 2005. Bayes empirical Bayes inference of amino acid sites under positive selection. *Molecular Biology and Evolution*, **22**(4): 1107–1118.
Yao TD, Liu XD, Wang NL, et al. 2000. Amplitude of climatic changes in Qinghai-Tibetan Plateau. *Chinese Science Bulletin*, **45**(13): 1236–1243.
Yu L, Wang XP, Ting N, et al. 2011. Mitogenomic analysis of Chinese snub-nosed monkeys: evidence of positive selection in NADH dehydrogenase genes in high-altitude adaptation. *Mitochondrion*, **11**(3): 497–503.
Zerbino DR, Birney E. 2008. Velvet: algorithms for de novo short read assembly using de Bruijn graphs. *Genome Research*, **18**(5): 821–829.
Zhang GJ, Li C, Li QY, et al. 2014. Comparative genomics reveals insights into avian genome evolution and adaptation. *Science*, **346**(6215): 1311–1320.
Zhang LW, He L, Hui M, et al. 2025. Evolutionary history and population dynamics of a widespread mantis shrimp *Oratosquilla oratoria*: evidence from mitogenomic analysis and species distribution modeling. *Regional Studies in Marine Science*, **81**: 104009.
Zhang XL, Ha BB, Wang SJ, et al. 2018. The earliest human occupation of the high-altitude Tibetan Plateau 40 thousand to 30 thousand years ago. *Science*, **362**(6418): 1049–1051.
Zhang Y, Wang J, Xiao Y. 2022. 3dRNA: 3D structure prediction from linear to circular RNAs. *Journal of Molecular Biology*, **434**(11): 167452.
Zheng GM. 2023. A Checklist on the Classification and Distribution of the Birds of China. 4th ed. Beijing: Science Press. (in Chinese)
Zheng WH, Li M, Liu JS, et al. 2014. Seasonal variation of metabolic thermogenesis in Eurasian tree sparrows (*Passer montanus*) over a latitudinal gradient. *Physiological and Biochemical Zoology*, **87**(5): 704–718.
Zhou TC, Shen XJ, Irwin DM, et al. 2014. Mitogenomic analyses propose positive selection in mitochondrial genes for high-altitude adaptation in galliform birds. *Mitochondrion*, **18**: 70–75.
Zink RM, Barrowclough GF. 2008. Mitochondrial DNA under siege in avian phylogeography. *Molecular Ecology*, **17**(9): 2107–2121.